

Performance Analysis of Open Loop V/f Control Technique for Six-Phase Induction Motor Fed By A Multiphase Inverter

Ahmet GÜNDOĞDU^{1*}, Reşat ÇELİKEL²

¹ Department of Electrical and Electronics Engineering, Faculty of Engineering, Batman University, Batman, Turkey
^{*1} ahmet.gundogdu@gmail.com, ² resat.celikel@batman.edu.tr

(Geliş/Received: 07/05/2020;

Kabul/Accepted: 22/08/2020)

Abstract: Due to its advantages such as high power density and low torque ripple, the multi-phase induction motors are preferred in high power industrial applications requiring wind turbines, in marine propulsion systems, and particularly in electric vehicles. Control of n-phase induction motor drive systems with nonlinear structure is performed scalar or vectorially. The scalar control technique, also called Volt/Hertz (V/f), has a simple mathematical model. For low-performance industrial applications, its applicability is easy and its cost is low. In terms of the microprocessor, it requires less operational load density. It is resistant against motor parameter changes. In this study, the open-loop speed control of a 6-phase induction motor with asymmetric winding structure was performed using the V/f control technique. The mathematical model of the 6-phase induction motor and the power circuit model of the 6-phase inverter were created in MATLAB/Simulink environment. Using the space vector pulse width modulation (SVPWM) technique, the stator voltage and stator frequency were controlled. In reference speed and load changes, transient and steady state performance analysis of the drive system was carried out. The obtained simulation results showed that the 6-phase induction motor could be successfully controlled by the V/f control technique.

Key words: Multiphase Motor, Six-Phase Motor, Multiphase Inverter, V/f Control, Space Vector PWM.

Çok Fazlı İnverterden Beslenen Altı Fazlı İndüksiyon Motorun Açık Çevrim V/f Kontrol Tekniğinin Performans Analizi

Öz: Çok fazlı indüksiyon motorlar yüksek güç yoğunluğu ve düşük moment dalgalanması gibi avantajlarından dolayı yüksek güç gerektiren endüstriyel uygulamalar ile rüzgâr türbinleri, gemi tahrik sistemleri ve özellikle de elektrikli araçlarda tercih edilmektedir. Doğrusal olmayan yapıya sahip n-fazlı indüksiyon motor sürücü sistemlerinin denetimi skaler veya vektörel olarak gerçekleştirilir. Volt/Hertz (V/f) olarak ta adlandırılan skaler kontrol tekniği basit bir matematiksel modele sahiptir. Düşük performanslı endüstriyel uygulamalar için uygulanabilirliği kolay ve maliyeti düşüktür. Mikroişlemci açısından daha az işlemsel yük yoğunluğu gerektirir. Motor parametre değişimlerine karşı dayanıklıdır. Bu çalışmada V/f kontrol tekniği kullanılarak asimetrik sargı yapısına sahip 6-fazlı bir indüksiyon motorun açık çevrim hız denetimi gerçekleştirilmiştir. 6-fazlı indüksiyon motorun matematiksel modeli ile 6-fazlı inverterin güç devresi modeli MATLAB/Simulink ortamında oluşturulmuştur. Uzay vektör darbe genişlik modülasyon tekniği (UVDGM) kullanılarak, stator gerilimi ve stator frekansı kontrol edilmiştir. Referans hız ve yük değişimlerinde, sürücü sistemin geçici ve sürekli durum performans analizi yapılmıştır. Elde edilen benzetim sonuçlarından 6-fazlı indüksiyon motorun, V/f kontrol tekniği ile başarılı bir şekilde kontrol edilebildiği gösterilmiştir.

Anahtar kelimeler: Çok Fazlı Motor, 6-Fazlı Motor, Çok Fazlı İnverter, V/f Kontrol, Uzay Vektör PWM.

1. Introduction

Alternating Current (AC) drives, developed to control induction motors commonly used in industrial applications, ensure the control of the speed, torque or rotor position of the motor at specified operating ranges. This control is generally performed vectorially or scalar. Induction motors have a complex structure whose parameters vary over time because of its mathematical model, and that contains nonlinear and high-order differential equations. Since there is no 90° phase difference between the components that make up the torque and the flux, they are not independent of each other and there is a clamping effect between them. The motor model has been developed as a result of the analytical analyses. With the development of the motor model, which would eliminate this clamping effect, the first study on vector-controlled AC drives was conducted by German engineer Blaschke in 1971 [1]. High-performance drives using Field Oriented Control (FOC) and Direct Torque Control (DTC) methods, known as *vector control* methods, are used successfully in the industrial field. The advantages and disadvantages of these methods, whose application schemes are different but purposes are

* Corresponding author: ahmet.gundogdu@gmail.com. ORCID Number of authors: ¹ 0000-0002-8333-3083, ² 0000-0002-9169-6466

the same, have been revealed by comparing from different angles [2]. The main purpose of both methods is to control the torque and flux of the motor independently of each other and without being affected too much by parameter changes.

In the control implementations performed with fixed-parameter controllers that are commonly used for this purpose, an accurate mathematical model of the drive system, which is being controlled, is required. The vector control method has high dynamic performance but is sensitive to changes in machine parameters. Determination of the amplitude and position of the flux vector in an accurate way plays an important role in the control process [3, 4]. In the *scalar control* method, on the other hand, the torque and flux cannot be controlled independently due to the magnetic coupling between the torque and flux components of the motor [5]. In the scalar control method, which has relatively lower performance, the controlled variables are only the stator voltage and frequency. Therefore, torque and flux are a function of these two variables and there is a magnetic coupling between them. This coupling effect causes the transient state performance of the motor to slow down and deteriorate. Oscillations occur in the torque. By keeping the ratio of the voltage and frequency (V/f) applied to the stator constant, the air-gap flux is kept constant and it is tried to ensure that the motor produces constant torque at all speed ranges [2].

However, at low speeds, since a significant portion of the source voltage falls on the stator resistance, the air-gap flux decreases despite the fact that the V/f ratio is constant. Because the stator voltage cannot be increased in the speed zone above the rated speed (i.e., in the field attenuation zone), the air-gap flux must be reduced. In both cases where field attenuation occurs, the motor moves out of the constant torque zone and continues to operate in the constant power zone, and thus the torque constancy of the motor is impaired. For this reason, scalar control method is not preferred in servo applications that require precise position control. However, this method is widely used in industrial applications that do not require high performance because it is easy to implement and cost effective [6,7]. It is resistant to changes in machine parameters. The scalar control method is performed as both open-loop and closed-loop. The open-loop V/f control method has poor dynamic performance and is low cost. However, changes in load torque result in a high-amplitude steady-state error at motor speed, and oscillations occur in the torque in the transient state. In applications requiring a fast dynamic response and more precise speed control, open-loop is insufficient and closed-loop V/f control method is preferred.

2. Multiphase Motors

Due to their advantages such as high torque density and low torque ripple, multi-phase induction motors are preferred in high-power industrial applications, wind turbines, marine propulsion system, and electric vehicles [8]. Multiphase machines have led the concept of the multiphase drive system to emerge. Although the concept of multiphase drive system entered the literature in the middle of the 20nd century, two studies that could be considered fundamental in this field were published at the beginning of this century. The first of these studies is related to the control of the 6-phase induction motor with asymmetric double winding structure [9]. The second, on the other hand, is the study in which a detailed literature review of multi-phase electrical machines used in variable speed applications is given [10]. When multi-phase machines are compared with three-phase machines, it is seen that they have higher reliability, higher torque density, lower torque ripple [11]. In addition, as the total power is divided by the number of phases, the power requirement of the multiphase machine per phase is reduced; thus, the current-voltage levels of the semiconductor switching elements that provide this power decrease.

Besides these advantages that they have, obtaining and controlling of their mathematical model is more complex and difficult [12]. Despite their complex structure, with the development of the inverter technology and modulation algorithms, control of multiphase electrical machines can be carried out easily via advanced control techniques. Despite the advantages and disadvantages mentioned above, it is seen clearly through the conducted literature review that the usage areas of multi-phase electrical machines have become widespread. In the industry, the profusion of three-phase motion systems and drives is remarkable. It can be said that interest in multi-phase induction motors and multi-phase motor drives, used especially in high power applications, has increased in the last three decades [13]. Among multi-phase induction motors, 6-phase induction motors are more preferred. These motors are classified in the literature under three main headings: a) Dual three-phase, b) Symmetric six-phase, c) Asymmetric six-phase. All three motor types consist of two three-phase windings and the layout of these windings is shown in Figure 1.

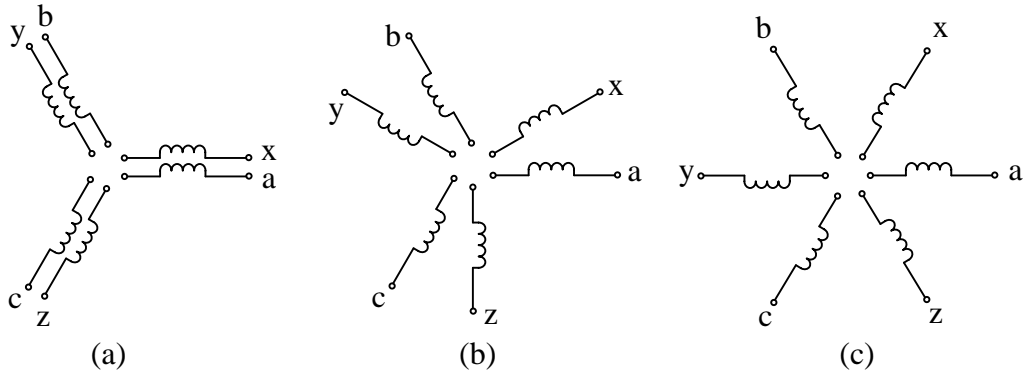


Figure 1. Winding layout of the 6-phase induction motor.

a) Dual three-phase ($\gamma = 0^\circ$), b) Asymmetric six-phase ($\gamma = 30^\circ$), c) Symmetric six-phase ($\gamma = 60^\circ$)

Some studies related to the control of 6-phase induction motors are given below. It was shown that the torque density of the motor was increased by adding the 3rd harmonic currents to the phase currents in the six-phase induction motor, and the results were supported by experimental studies [14]. An experimental study in which two separate three-phase inverters were used for indirect field-oriented control of six-phase induction motors was conducted [15]. Field-oriented vector control of six-phase induction motors consisting of two separate three-phase windings with an electrical angle of 30° between them was experimentally performed using six-phase inverters [16]. Rotor-field-oriented vector control of a six-phase induction motor with 10 kW power was performed experimentally [17]. Harmonic analysis of the windings of a 4-pole, 48-slot six-phase induction motor for open and short circuit states was performed both by simulation and experimentally and the results were compared [18]. Efficiency and performance analysis of high-frequency three-phase and six-phase induction motors used in medium and low power applications were performed. The results obtained by simulation and experimentation were given comparatively [19]. A new control algorithm that reduced torque ripples and motor losses in the motor in conditions where one or more of the motor phase windings were open-circuit was proposed. The validity of the proposed method was confirmed experimentally [20].

A new SVPWM technique was proposed to control a 15 kW six-phase induction motor, consisting of two separate three-phase windings, via a six-phase inverter. Though this proposed new technique was easy to implement digitally, it significantly reduced the harmonic current components of stator currents. The study was validated with experimental results [21]. Detailed mathematical models of two separate five-phase and six-phase motor drive systems were created for steady-state operation. The experimental results were given comparatively [22]. For current control of the six-phase induction motor with asymmetric winding structure, the model-based predictive control method was experimentally analyzed. Simulations were made to examine the performance of the control method. To determine the performance of the model-based predictive control method, the effect of the number of the considered voltage vectors was investigated and different cost functions were analyzed. The calculation time required to prove the real-time applicability of the control method was discussed [23]. By the field-oriented control method in which two separate controller structures (Fuzzy Controller-FC and sliding mode-SM controllers) were used, the vector control of the six-phase induction motor was performed experimentally. Analyses were made for the condition where three of the motor phase windings were open-circuit or disabled [24]. Direct torque control of the six-phase induction motor was performed without using a speed measurement sensor [25]. A new flux controller based on “adaptive gradient descent” was proposed to increase the efficiency of the six-phase induction motor controlled by the direct torque control method. It was validated by experimental studies that the proposed controller greatly increases efficiency by reducing iron losses and harmonic losses. This new controller structure is easy to implement, adaptable, and also requires no additional hardware for practical applications [26].

An experimental study was conducted on different current control techniques in the six-phase induction motor drive system with asymmetric winding structure [27]. Sensorless control of the six-phase induction motor with asymmetric winding structure was performed using the “non-linear backstepping control” method. Speed and voltage sensors were not used in the control algorithm [28]. In another study, a compilation of the studies conducted until 2016 and 2018 was given respectively [29, 30]. A “Circuit-Oriented Method” based motor model was developed to simulate possible failure conditions on the stator and rotor sides. The performance of

the model was observed both by simulation and experimentally using a 90-w, 14-V, 50-Hz, bipolar six-phase induction motor. Results were given comparatively [31]. The speed and torque control of the six-phase induction motor fed by a two-level six-phase inverter was experimentally performed using the direct torque control method. With the developed voltage-vector-selection algorithm, ripples in motor torque were reduced [32]. A detailed experimental analysis related to the failure conditions of six-phase induction motors with asymmetric, symmetrical and dual three-phase winding structures was conducted [33]. Blank operation and locked-rotor tests of the six-phase induction motor with an asymmetric winding structure were performed and motor parameters were estimated. To increase the accuracy of predicted parameters, a zero-sequence test method using an improved equivalent circuit was proposed. The proposed method was validated using experimental results [34].

For the creation of virtual voltage vectors used to reduce current harmonics, a simplified method was proposed. The proposed method was validated using experimental results [35]. A new prediction algorithm based on Model Reference Adaptive System-MRAS was proposed to predict and monitor stator resistance online. Direct torque control of the six-phase induction motor was performed experimentally by the proposed prediction algorithm [36]. For speed-sensorless direct torque control of a six-phase induction motor, a second-order sliding-mode MRAS-based flux observer was proposed. The performance of the proposed observer was validated by experimental results [37]. In six-phase induction motors, the effects of harmonics induced in the air-gap on the dynamic behavior of the motor were investigated. With the developed space harmonic model, analyses were made for both normal operation and fault states. The proposed model was experimentally performed using a 1.5 kW six-phase induction motor [38].

3. Mathematical Model of 6-Phase Induction Motor

The six-phase induction motor is a 6-dimensional system. Therefore, modeling and controlling of the motor in the original 6-phase reference plane is very difficult. In the general machine theory, mathematical transformations are used to facilitate the solution of differential equations whose coefficients vary over time and whose solution is difficult, and to reduce all variables to a common reference frame. If these transformations are used, the coupling effect between some variables is eliminated and a simplified model of the machine is obtained. To establish a dynamic model of these motors, the concepts of $\alpha\beta$ and dq conversion used in the derivation of the 2-phase equivalent circuit model of a 6-phase source-fed motor need to be known and properly laid out. In the 6-phase induction motor with asymmetric winding structure, two 3-phase windings are placed in the stator as shown in Figure 2 in a way that there is $\gamma=30^\circ$ electrical angle between them. The windings are star-connected and neutral points are insulated from each other [39].

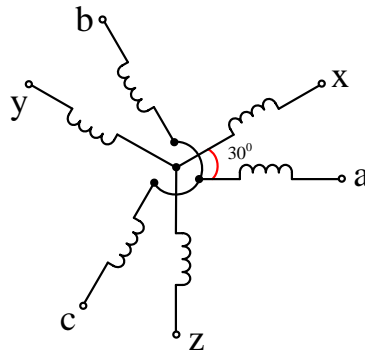


Figure 2. Asymmetric winding layout.

The mathematical model of these two winding groups, which are separated from each other by an electrical angle $\gamma=0$, in the $\alpha\beta$ axis set is given by the following equations. While modeling, it was assumed that stator windings were distributed as sinusoidal around air-gap, that air-gap flux showed a uniform distribution, that friction, ventilating losses and magnetic saturation were neglected, and that the windings were identical. If $p = d/dt$;

Voltage equations;

$$V_{s\alpha} = R_s I_{s\alpha} + p\lambda_{s\alpha} \quad (1)$$

$$V_{s\beta} = R_s I_{s\beta} + p\lambda_{s\beta} \quad (2)$$

$$V_{r\alpha} = R_r I_{r\alpha} + p\lambda_{r\alpha} + \omega_r \lambda_{r\beta} = 0 \quad (3)$$

$$V_{r\beta} = R_r I_{r\beta} + p\lambda_{r\beta} - \omega_r \lambda_{r\alpha} = 0 \quad (4)$$

where the notations of "s" and "r" refer to the stator and rotor variables, respectively. In addition, while the stator voltages are referred by $V_{s\alpha}$ and $V_{s\beta}$, $I_{s\alpha}$ and $I_{s\beta}$ refer to stator currents, $I_{r\alpha}$ and $I_{r\beta}$ refer to rotor currents. ω_r is rotor angular speed. R_s , R_r are stator and rotor winding resistances respectively.

Flux equations;

$$\lambda_{s\alpha} = \int (V_{s\alpha} - R_s I_{s\alpha}) dt \quad (5)$$

$$\lambda_{s\beta} = \int (V_{s\beta} - R_s I_{s\beta}) dt \quad (6)$$

$$\lambda_{r\alpha} = \int (-R_r I_{r\alpha} - \omega_r \lambda_{r\beta}) dt \quad (7)$$

$$\lambda_{r\beta} = \int (-R_r I_{r\beta} + \omega_r \lambda_{r\alpha}) dt \quad (8)$$

Current equations;

$$I_{s\alpha} = (L_r \lambda_{s\alpha} - L_m \lambda_{r\alpha}) / (L_s L_r - L_m L_m) \quad (9)$$

$$I_{s\beta} = (L_r \lambda_{s\beta} - L_m \lambda_{r\beta}) / (L_s L_r - L_m L_m) \quad (10)$$

$$I_{r\alpha} = (L_s \lambda_{r\alpha} - L_m \lambda_{s\alpha}) / (L_s L_r - L_m L_m) \quad (11)$$

$$I_{r\beta} = (L_s \lambda_{r\beta} - L_m \lambda_{s\beta}) / (L_s L_r - L_m L_m) \quad (12)$$

where $\lambda_{s\alpha}$, $\lambda_{s\beta}$ are stator flux components, $\lambda_{r\alpha}$, $\lambda_{r\beta}$ are rotor flux components. L_s , L_r are stator and rotor inductances and L_m is mutual inductance.

Electromagnetic torque equation;

$$T_e = (3P/2)L_m [I_{s\beta} I_{r\alpha} - I_{s\alpha} I_{r\beta}] \quad (13)$$

The relationship between the mechanical speed of the motor and its electrical speed is expressed as in Equation 14 by taking into account the number of poles of the motor.

$$J \frac{2}{P} \frac{d\omega_r}{dt} = T_e - T_L - \frac{2}{P} B \omega_r \quad (14)$$

where J is the moment of inertia of the motor (kg.m²) and B is the coefficient of friction that causes the moment of friction (Nm.s). The MATLAB/Simulink model in the $\alpha\beta$ axis set of the 6-phase induction motor with

asymmetric winding structure given above equations was formed as in Figure 3. The V/f control of the motor whose simulation model was formed described in detail in section 4.

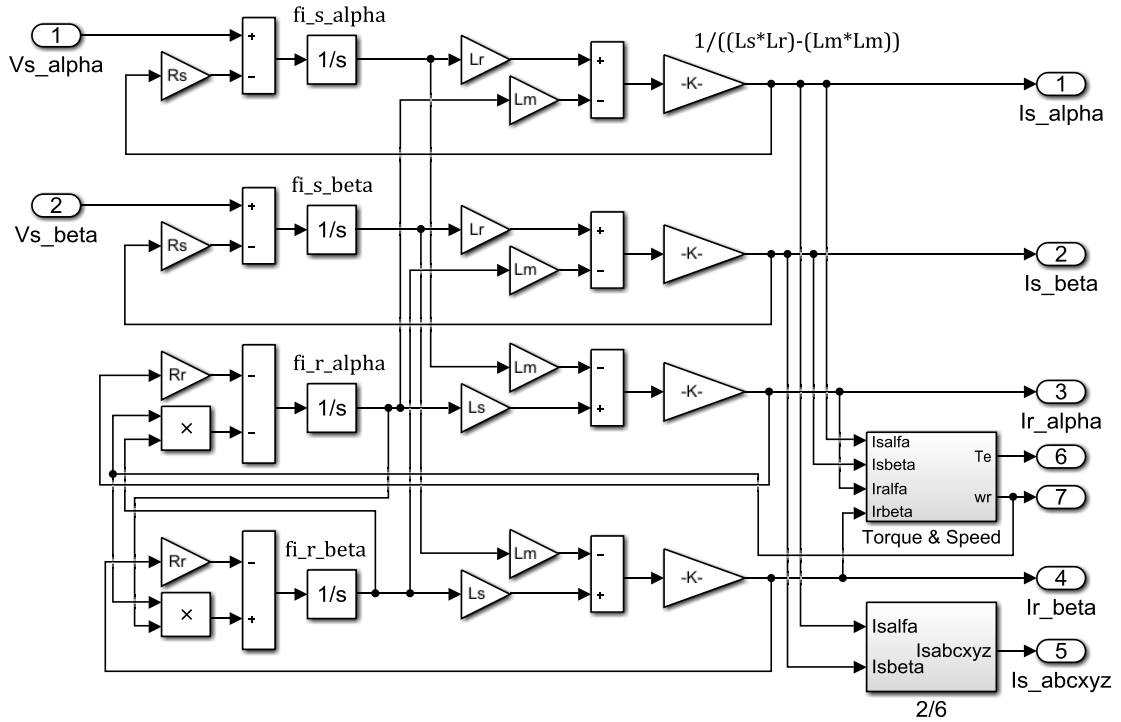


Figure 3. 6-phase induction motor's MATLAB/Simulink model in $\alpha\beta$ axis.

4. V/f Control of 6-Phase Induction Motor

The speed and torque response of an induction motor controlled by the V/f scalar control method is low due to the clamping effect between the flux and torque components. As a result of analytical analysis on the motor model, this clamping effect is eliminated based on the development of the motor Model, which is represented by space vectors reduced to two axes, instead of n-number phase variables. Thus, the flux and torque of the motor can be controlled independently from each other. By eliminating the clamping effect, the speed and torque response of the motor is improved. With the development of this method, known as vector control, it has been understood that this low speed and torque response in the scalar control method is not due to the structure of the induction motor, but it is due to the form of the control applied to the motor [40,41].

The V/f control method is one of the methods used in the control of the variable-speed industrial drive systems. Its structure is simple and its cost is low. It can be performed as open and closed loop. The V/f method is a method based on the variation of the amplitude and frequency of the stator voltage of the motor. In induction motors, rotor speed is a function of the stator frequency. Therefore, in order to reach the desired rotor speed in the variable speed applications, the frequency of the stator voltage must be re-determined for each speed value. In order for the motor to produce constant torque at all speed values up to nominal speed, the motor's air-gap flux (λ_s) must be kept constant. However, by keeping the stator voltage constant, only changing the frequency of it distorts the stability of the air-gap flux. The generation of the torque in the motor depends on the formation of flux. The relationship between stator voltage and stator flux is given in Equation 15.

$$V_{s\alpha} = R_s I_s + p \lambda_s \quad (15)$$

The stator flux is defined as the integral of the back-emf voltage induced in the stator windings, and it is calculated as in Equation 16.

$$\lambda_s = \int (V_s - R_s I_s) dt \quad (16)$$

If the ohmic voltage drop up to $R_s I_s$ on the stator winding resistance is ignored, then Equation 17 is obtained.

$$\lambda_s = \int V_s dt \quad (17)$$

As can be seen in Equation 17, the stator flux vector λ_s is the integral of the applied V_s voltage and it is also directly related to the amplitude and frequency of that voltage. The impedance of the motor winding to which the V_s voltage is applied is $Z = \sqrt{R^2 + (X_L)^2}$. Here, $X_L = 2\pi f_s L$ is the inductive reactance of the winding and it is directly related to the frequency of the applied voltage f_s . In the V/f control method; 1) Changing only the f_s frequency by keeping the V_s winding voltage constant changes both the inductive reaction of the winding (X_L) and the total winding impedance (Z). Since the winding current I_s will change accordingly, the stator flux λ_s also changes. 2) If the f_s stator frequency is kept constant and only the V_s voltage is changed, again, the stator flux λ_s changes. Therefore, in order for the controlled motor to operate under constant torque at different speed values, the stator voltage and the stator frequency must be changed together. Because of this, in order to generate constant torque with constant λ_s flux in the motor, the voltage/frequency ratio must be kept constant. This ratio, known as the V/f ratio, is formulated with $k = V_s/f_s$.

As known, the T_e electromagnetic torque generated by the motor is as much as the ratio of the power of the motor to the mechanical speed of the motor and is expressed by Equation 18.

$$T_e = \frac{P_e}{\omega_m} \quad (18)$$

where ω_m is the mechanical speed of the motor. P_e is the power generated by the motor. Assuming that P is the number of poles, there is a relationship in the form $\omega_m = 2\omega_r/P$ between the mechanical speed of the motor and its electrical speed. Taking this relationship into account, a general diagram of the V/f method can be given as in Figure 4.

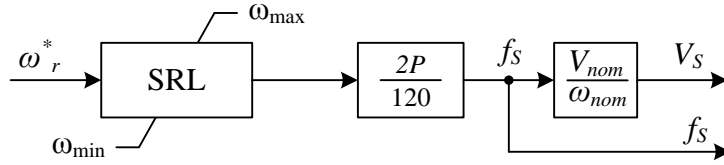


Figure 4. General principle diagram of V/f.

With the reference speed information at the block input shown in Figure 4, first the stator frequency f_s , then by multiplying this frequency value by the constant k , the stator voltage V_s corresponding to this frequency is calculated. The V_s and f_s obtained from the block output are the reference signals used to obtain the V_α and V_β voltages at the input of the SVPWM modulation algorithm that will drive the inverter, and these are recalculated for each reference speed value. Due to the clamping effect between the torque and flux components of the motor, the transient state performance of the V/f control technique is low. Against sudden reference speed changes, the motor cannot respond dynamically quickly enough. Therefore, in the transient state zone, the dynamic performance of the motor can be partially controlled using the slew rate limiter (SRL) block. The SRL block ensures delay only at sudden reference speed changes on a specific slope.

5. Space Vector Pulse Width Modulation (SVPWM)

In order for the V/f control of the 6-phase induction motor to be performed, the power supply feeding the motor must be a controlled-source whose voltage and frequency can be changed. In this study, the power circuit model of the 6-phase inverter used as a controlled power supply is given in Figure 5. In the control process, a 6-phase inverter with a single DC bus bar structure given in Figure 5 can be used, as well as two separate 3-phase

inverters can also be used. In high-power drive systems where 6-phase inverters with a single DC bus bar structure are used, the design of the DC bus bar is of particular importance.

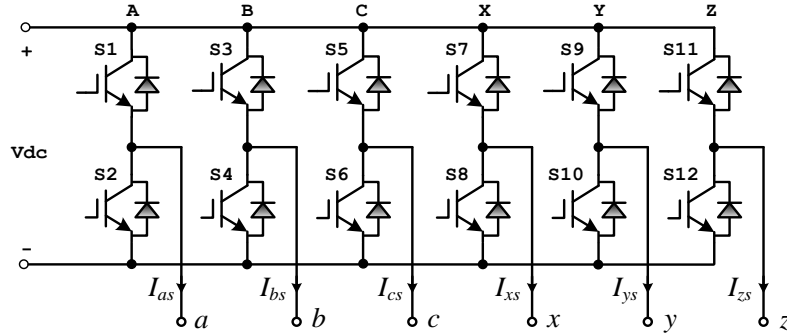


Figure 5. Power circuit model of the 6-phase inverter.

In Figure 5, the *abc* ends at the output of the inverter, which will feed the motor, feed the first 3-phase winding group of the motor, while the *xyz* ends feed the second 3-phase winding group. Between the current and voltages of these winding groups, which are placed separately with 30° electrical angles into the stator, there must also be 30° electrical angles. Therefore, for modulation of the inverter legs feeding each winding group, two separate SVPWM switching blocks whose input signals are separated 30° were used. The block diagram related to this is given in Figure 6.

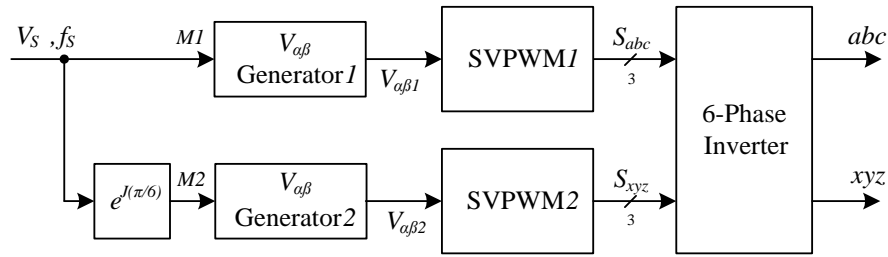


Figure 6. General principle diagram of V/f control of 6-phase induction motor.

6. V/f Drive System Model of 6-Phase Induction Motor

A general block diagram for the drive system is given in Figure 7. In the drive system performed as open loop, V_α and V_β input voltage values of the SVPWM algorithm were obtained from the reference speed input. The SVPWM1 block generates the triggering signals of switches on the ABC legs of the 6-phase inverter, while the SVPWM2 block generates the triggering signals of the switches on the XYZ legs. For both modulation algorithms, the switching frequency was chosen as $f_s = 5 \text{ kHz}$.

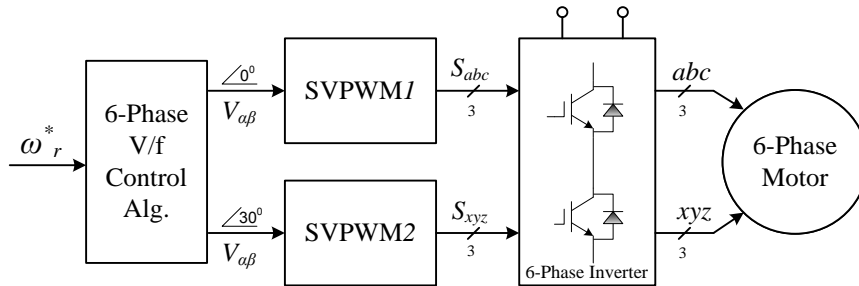


Figure 7. V/f drive system model of the 6-phase induction motor.

7. Simulation of V/f Speed Control of 6-Phase Induction Motor With MATLAB/Simulink

In this section, the open-loop V/f control of the 6-phase induction motor fed from the 6-phase inverter was simulated with MATLAB/Simulink. The simulation model for this is given in Figure 8.

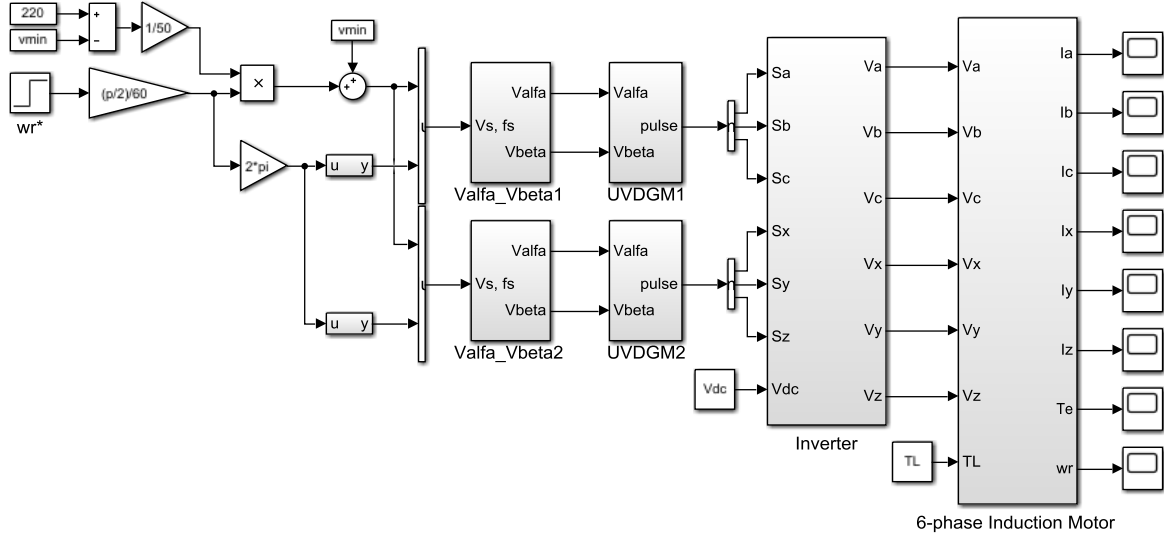


Figure 8. MATLAB/Simulink model of open-loop V/f control of 6-phase induction motor.

Within the Model, the V/f ratio was obtained first, and then the effective value of the V winding voltage required by the motor windings was determined by multiplying the obtained V/f ratio by the f frequency information generated from the reference speed information. The variation of M1 modulation signal in 0° plane and M2 modulation signals in 30° plane obtained by using this voltage and frequency information, which should be applied to Stator windings, is given in Figure 9.

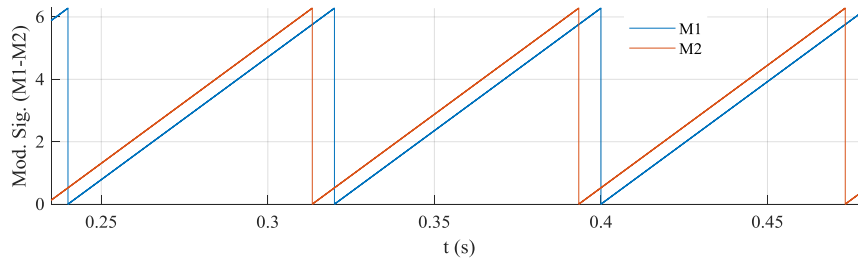


Figure 9. Change of M1-M2 modulation signals.

At low reference speed values, the frequency and voltage values generated by the algorithm will be low due to the constant V/f ratio. At low stator voltages, the motor will not be able to generate sufficient startup torque since a large part of the source voltage will fall as $R_s I_s$ on the stator winding. Therefore, in low-speed zones, the minimum boost voltage must be applied to the motor windings in order for the motor to generate sufficient startup torque.

8. Simulation Results

The simulation results obtained for different speed and load values by using the simulation model in Figure 8 are given with the following graphs. In Figure 10, for the reference speeds given as +750 rpm and +1500 rpm in the case of no-load operation, motor speed, motor torque, stator one phase winding current, and changes in the amplitude of the stator flux consisting of the components $\alpha\beta$ are given, respectively. In Figure 10a, the motor follows the given reference speeds properly. Within reference speeds capture times, the motor reaches the

steady-state by generating a torque worth of V/f ratio. In the reference speed changes, motor speed to reach the reference speed times are high due to the open-loop control structure and its transient state performance is low. This is a natural result of the open-loop V/f control algorithm. For further improvement of the transient state performance, closed-loop V/f control technique may be preferred. Thus, by processing the speed error between the reference speed and the actual speed taken from the motor shaft by a PI speed controller, it is ensured the motor to generate maximum torque. The fact that the motor generate maximum torque at reference speed changes further shortens the actual motor speed to reach reference speed (settling time), thus increases the motor's transient state performance.

In Figure 10b, it is seen that the motor generates high torque in the transient state to capture the given reference speeds and that in the steady state zone at constant speeds, the motor generates enough torque to meet the idle iron, friction and ventilating losses. As shown in Figure 10c, for the same reference speed values, the motor one phase winding current is higher in the transient state, and in the steady state, on the other hand, it is at the value that can generate the idle running torque of the motor. Since the V/f ratio is equal and constant at both reference speed values, the motor phase winding current has the same amplitude in both steady states except the transient state. Figure 10d shows the change in amplitude of the stator flux formed by $\alpha\beta$ flux components. Since the V/f ratio is equal and constant at both reference speed values, the stator flux is constant and has the same amplitude in both constant speed regions except the transient state. The fact that the stator flux has the same amplitude at different speed values means that the motor generates constant torque. For this reason, this region where the constant V/f ratio and the stator flux are kept constant from zero to nominal speed is called the *constant torque region*.

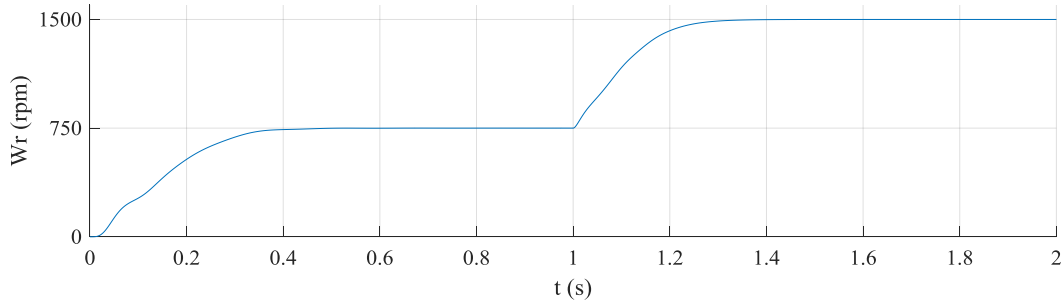


Figure 10a. Rotor speed at no-load operating state for +750 rpm to +1500 rpm.

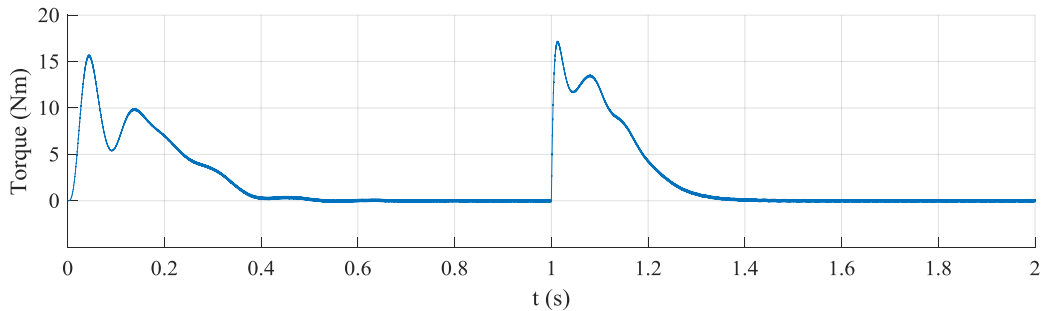


Figure 10b. Motor torque at no-load operating state for +750 rpm to +1500 rpm.

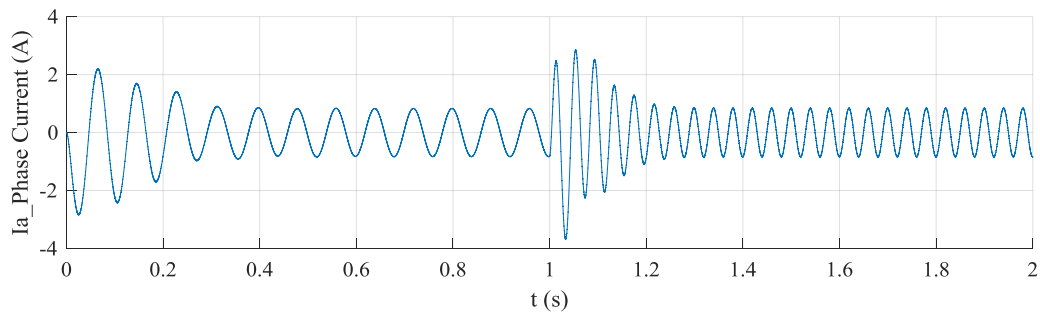


Figure 10c. Stator phase winding current at no-load operating state for +750 rpm to +1500 rpm.

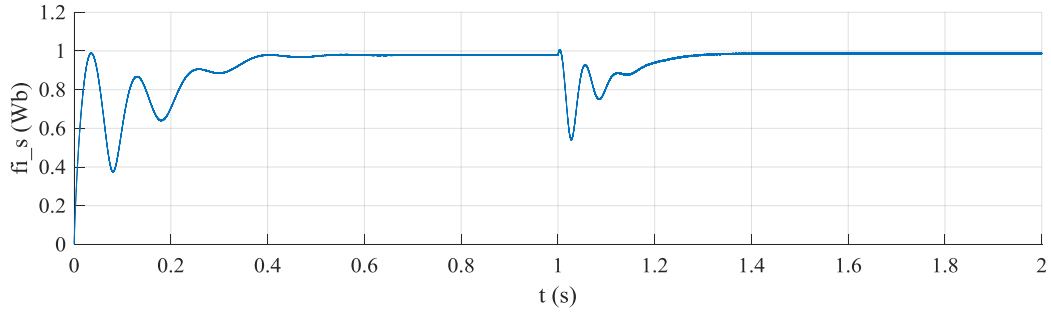


Figure 10d. Stator flux at no-load operating state for +750 rpm to +1500 rpm

Figure 11 presents stator currents at reference speeds given as +750 rpm and +1500 rpm in the case of no-load operation. Figure 11a shows stator currents at +750 rpm reference speed and Figure 11b shows stator currents at 1500 rpm reference speed. The 6-phase stator currents in both graphs are of the same amplitude; however, the frequency of stator currents obtained for the reference speed of +750 rpm is lower than the frequency of stator currents obtained at +1500 rpm speed.

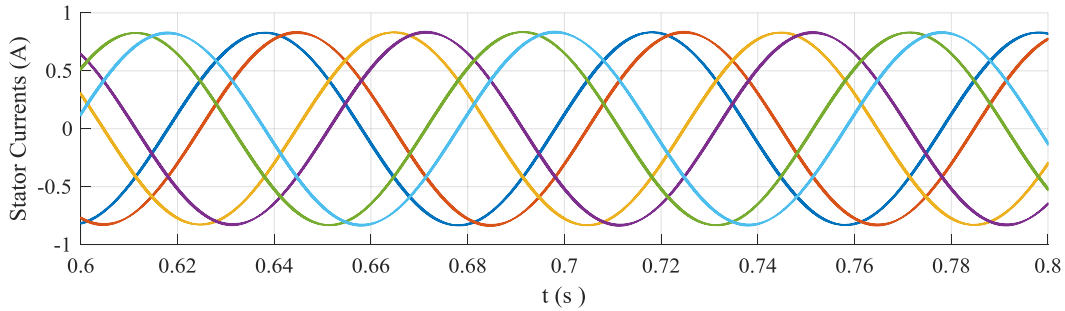


Figure 11a. Stator currents at no-load operating state for +750 rpm.

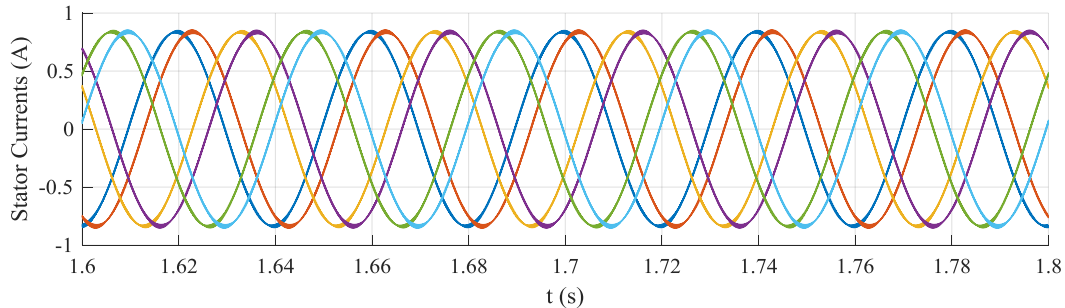


Figure 11b. Stator currents at no-load operating state for +1500 rpm.

In Figure 12-abcd, graphs for the on-load operating state at 1400 rpm are given. In the range of 0.8 to 1.2 sec, the motor was loaded with 4 Nm. In Figure 12a, a decrease in motor speed with loading was observed. The slip amount increased with loading and the motor continued to operate with steady-state speed error throughout the loading period. Steady-state speed error is one of the major disadvantages of open-loop control systems. In order for the decreasing motor speed to capture the reference speed again, the amount of slip must be compensated by the V/f algorithm. This compensation process is possible by feeding of the measured rotor speed back into the algorithm. The increased motor torque, motor currents and stator flux during the same loading period are shown in figures 12b,c,d, respectively.

As seen in Figure 12b, the motor generated a torque, which was in value that could meet the load imposed on its shaft during the loading period. Depending on the decreasing rotor speed and increased slip along with loading, the amplitude and frequency of the induced tension on the rotor increases. This causes the rotor flux λ_r to increase. As required by equation 9 and equation 10, the increased rotor flux also increases the stator currents. The increase of stator currents is shown in Figure 12c. On the other hand, as required by Equation 5 and

Equation 6, the increase of the stator current under constant V_s stator voltage causes the stator flux to decrease. This decrease in the stator flux is shown in Figure 12d.

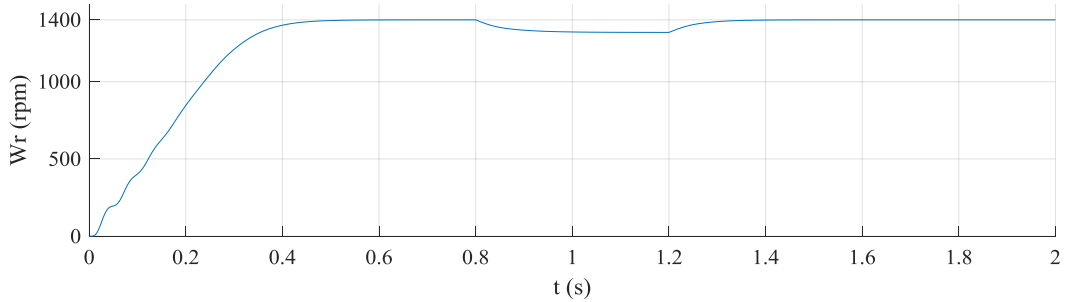


Figure 12a. Rotor speed at the loaded state.

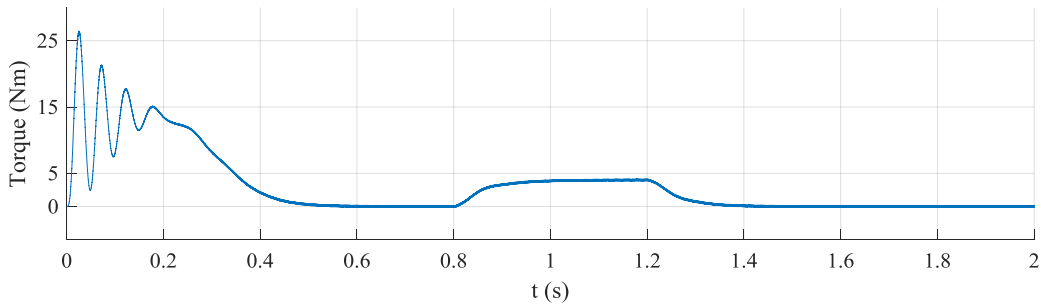


Figure 12b. Motor torque at the loaded state.

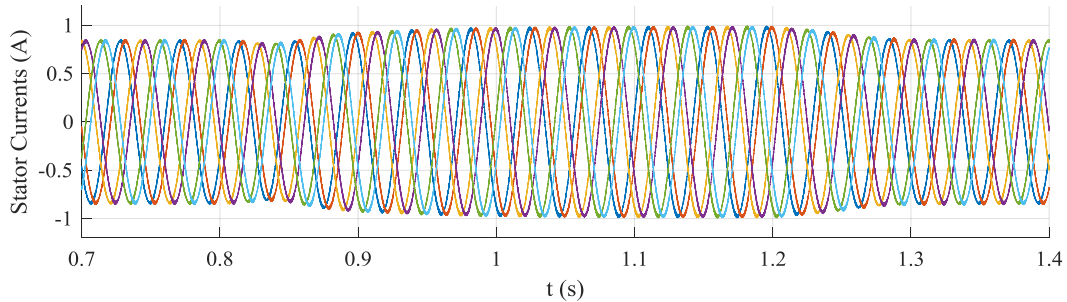


Figure 12c. Stator phase currents at the loaded state.

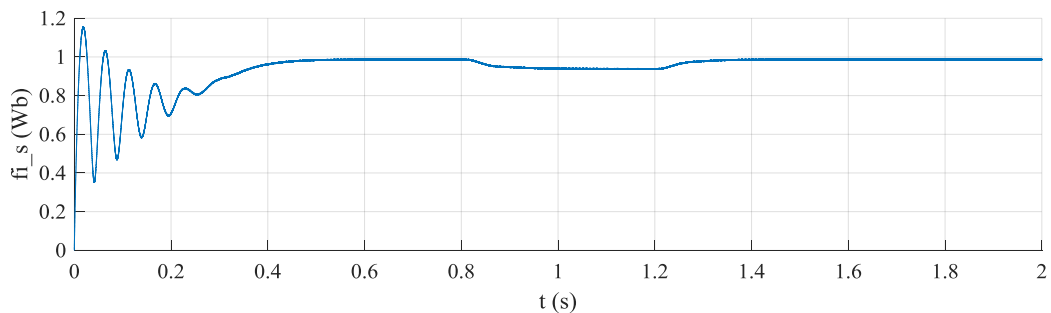


Figure 12d. Variation of the amplitude of the stator flux at the loaded state.

Figure 13-a,b,c,d show the speed, current, torque and flux graphs in the change of reference speed from +1500 rpm to -1500 rpm at the unloaded state. As can be seen from the graphs, in the region where the reference speed changes, the motor has generated maximum torque by drawing maximum current from the source. In Figure 13b, six-phase stator currents, and in Figure 13c, motor torque are shown. The decrease in stator flux within the time of settling on the reference speed in the negative direction is seen in Figure 13d.

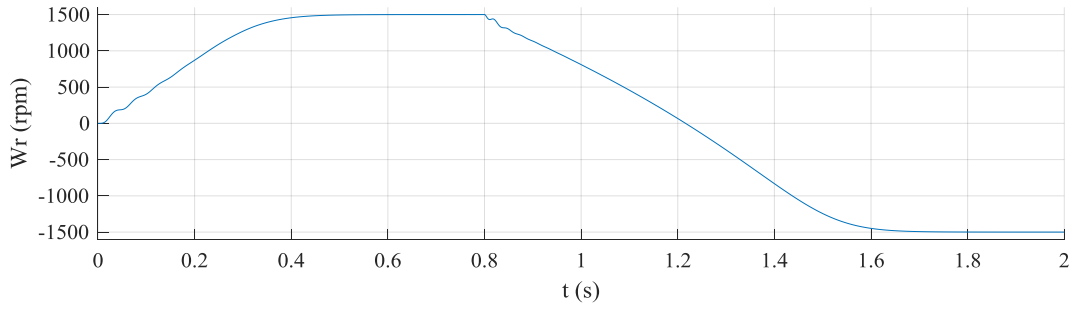


Figure 13a. Rotor speed.

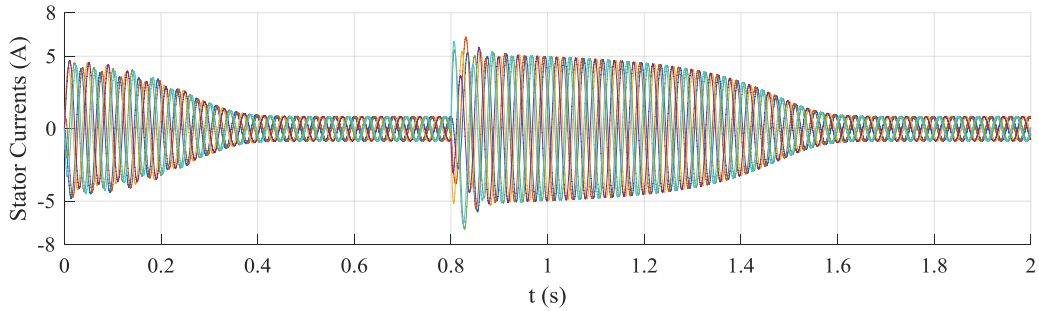


Figure 13b. 6-phase stator currents.

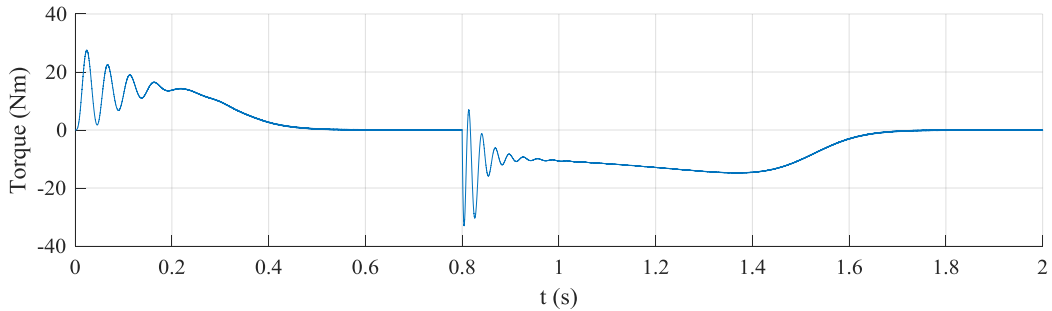


Figure 13c. Motor torque.

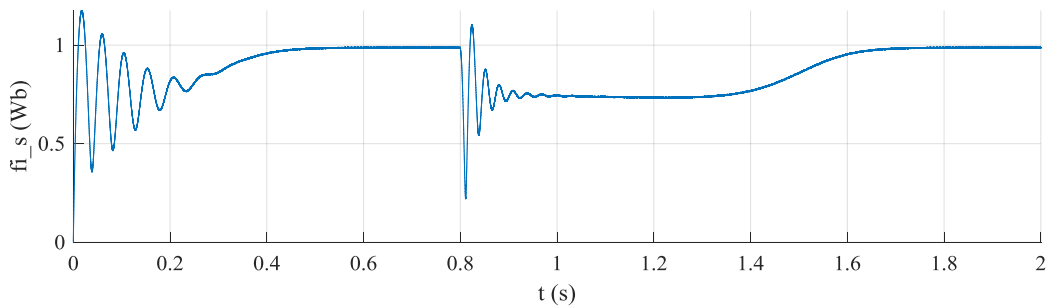


Figure 13d. Stator flux.

9. Conclusion

Due to its easy applicability and low cost, the open-loop V/f control method is preferred for low-performance industrial applications. In this study, open-loop speed control of a 6-phase induction motor with asymmetric winding structure was performed in MATLAB/Simulink environment by using the V/f control technique. A 6-phase induction motor was preferred because of its advantages such as high reliability, high torque density, and low torque ripple compared to 3-phase induction motors. With the conducted simulation studies, it was shown that the 6-phase induction motor could be successfully controlled by the V/f control technique.

Since the speed feedback is not used in the drive system realized as open-loop, the transient state performance of the motor is low in terms of the time to reach the reference speed. In addition, in the case of loaded operation, the steady-state speed error occurs in proportion to the magnitude of the load torque. This is a natural result of the open-loop V/f control technique and is not due to the structure of the motor. On the other hand, the motor's steady-state performance in the no-load and four-quadrant operation modes is high. In the drive systems where 6-phase induction motors are used, since the total power is divided by the number of phases, the current, voltage and power requirements per phase decrease. Therefore, drive circuit design can be realized with semiconductor switching elements with lower current and voltage capacity. It is thought that the 6-phase induction motor, controlled by advanced control methods, may be an alternative to the permanent magnet synchronous motors commonly used in electric vehicles.

Appendix A

Motor Parameters:

$R_s=10.1 \Omega$; $R_r=9.8546 \Omega$; $L_s=0.8330 \text{ H}$; $L_r=0.8330 \text{ H}$; $L_m=0.7827 \text{ H}$; $J=0.06 \text{ kg.m}^2$; $B=0 \text{ Nm.s}$; $P=4$;

Rated Values:

$V_{\text{phase}}=220 \text{ V}$, $V_{\text{line}}=380 \text{ V}$, $V_{\text{dc}}=537 \text{ V}$, $V_{\text{boost}}=V_{\text{min}}=30 \text{ V}$, $P=550 \text{ W}$, $T=4 \text{ Nm}$.

References

- [1] Blaschke F. A New Method for the Structural Decoupling of AC Induction Machines. In Conf. Rec. IFAC, Dusseldorf, Germany 1971; 1-15.
- [2] Hoang L.H. Comparison of Field-Oriented Control and Direct Torque Control for Induction Motor Drives. Thirty-Fourth IAS Annual Meeting. Conference Record of the 1999; IEEE Industry Applications Conference, 2: 1245-1252.
- [3] Siddavatam R, Prakash R, Umanand L. Improving the Dynamic Response of Scalar Control of Induction Machine Drive using Phase Angle Control. IECON 2018-44th Annual Conference of the IEEE Industrial Electronics Society. 541-546.
- [4] Gündoğdu A, Dandil B, Ata F. Direct Torque Control Based on Hysteresis Controller of Asynchronous Motor. Science and Engineering Journal of Firat University 2017; 29(1): 197-205.
- [5] Altay AS. Sensorless Vector Control Of a Three Phase-Induction Motor By Using a New MRAS Method. Phd.Thesis, İstanbul Technic University Institute of Science, İstanbul, (2014).
- [6] Sen PC. Electric Motor Drives and Control Past Present, and Future”, IEEE Transactions on Industrial Electronics 1990; 37(6): 562-575.
- [7] Bose BK. Modern Power Electronics and AC Drivers, Prentice Hall, New Jersey, (2002).
- [8] Levi E, Barrero F, Duran MJ. Multiphase Machines and Drives-Revisited. IEEE Transactions On Industrial Electronics 2016; 63(1): 429-432.
- [9] Bojoi R, Farina F, Profumo F, Tenconi A. Dual-three phase induction machine drives control—a survey. IEEJ Transactions on Industry Applications 2006; 126(4): 420-429.
- [10] Levi E. Multiphase electric machines for variable-speed applications. IEEE Transactions on Industrial Electronics 2008; 55(5): 1893-1909.
- [11] Levi E, Bojoi R, Profumo F, Toliyat HA, Williamson S. Multiphase Induction Motor Drives-a Technology Status Review. IET Electr. Power Appl., 2007; 1(4): 489–516.
- [12] Hou L, Su Y, Chen L. Dsp-Based Indirect Rotor Field Oriented Control for Multiphase Induction Machines. IEEE Int. Electric Machines and Drives Conference 2003; 976-980.
- [13] Jones M, Vukosavic S, Levi E, Iqbal A. A Six-Phase Series- Connected Two-Motor Drive With Decoupled Dynamic Control. IEEE Transactions on Industry Applications 2005; 41(4): 1056-1066.
- [14] Lyra ROC, Lipo TA. Torque Density Improvement in a Six-Phase Induction Motor With Third Harmonic Current Injection. IEEE Transactions On Industry Applications 2002; 38(5): 1351-1360.
- [15] Singh GK, Nam K, Lim SK. A Simple Indirect Field-Oriented Control Scheme for Multiphase Induction Machine. IEEE Transactions On Industrial Electronics 2005; 52(4): 1177-1184.
- [16] Mohapatra KK, Kanchan RS, Baiju MR, Tekwani PN, Gopakumar K. Independent Field-Oriented Control of Two Split-Phase Induction Motors From a Single Six-Phase Inverter. IEEE Transactions On Industrial Electronics 2005; 52(5): 1372-1382.
- [17] Bojoi R, Levi E, Farina F, Tenconi A, Profumo F. Dual three-phase induction motor drive with digital current control in the stationary reference frame. IEE Proc.-Electr. Power Appl., 2006; 153(1): 129-139.
- [18] Apsley J, Williamson S, Analysis of Multiphase Induction Machines With Winding Faults. IEEE Transactions On Industry Applications 2006; 42(2): 465-472.
- [19] Boglietti A, Bojoi R, Cavagnino A, Tenconi A. Efficiency Analysis of PWM Inverter Fed Three-Phase and Dual Three-Phase High Frequency Induction Machines for Low/Medium Power Applications. IEEE Transactions On Industrial Electronics 2008; 55(5): 2015-2023.

- [20] Kianinezhad R, Nahid-Mobarakeh B, Baghli L, Betin F, Capolino GA. Modeling and Control of Six-Phase Symmetrical Induction Machine Under Fault Condition Due to Open Phases. *IEEE Transactions On Industrial Electronics* 2008; 55(5): 1966-1977.
- [21] Marouani K, Baghli L, Hadiouche D, Kheloui A, Rezzoug A. A New PWM Strategy Based on a 24-Sector Vector Space Decomposition for a Six-Phase VSI-Fed Dual Stator Induction Motor. *IEEE Transactions On Industrial Electronics* 2008; 55(5):1910-1920.
- [22] Levi E, Jones M, Vukosavic SN, Toliyat HA. Steady-State Modeling of Series-Connected Five-Phase and Six-Phase Two-Motor Drives. *IEEE Transactions On Industry Applications* 2008; 44(5): 1559-1568.
- [23] Barrero F, Arahal MR, Gregor R, Toral S, Duran MJ. A Proof of Concept Study of Predictive Current Control for VSI-Driven Asymmetrical Dual Three-Phase AC Machines. *IEEE Transactions On Industrial Electronics* 2009; 56(6): 1937-1954.
- [24] Fnaiech MA, Betin F, Capolino GA, Fnaiech F. Fuzzy Logic and Sliding-Mode Controls Applied to Six-Phase Induction Machine With Open Phases. *IEEE Transactions On Industrial Electronics* 2010; 57(1): 354-364.
- [25] Zaimeddine R, Undeland T. Direct Torque Control Scheme For Dual-Three-Phase Induction Motor. *The 2010 International Power Electronics Conf.*, 2010; 3007-3014.
- [26] Taher A, Rahmati A, Kaboli S. Efficiency Improvement in DTC of Six-Phase Induction Machine by Adaptive Gradient Descent of Flux. *IEEE Transactions On Power Electronics* 2012; 27(3): 1552-1562.
- [27] Che HS, Levi E, Jones M, Hew WP, Rahim NA. Current Control Methods for an Asymmetrical Six-Phase Induction Motor Drive. *IEEE Transactions On Power Electronics* 2014; 29(1): 407-417.
- [28] Seyed M, Fatemi JR, Abjadi NR, Soltani J, Abazari S. Speed sensorless control of a six-phase induction motor drive using backstepping control. *IET Power Electronic* 2013; 7(1): 114–123.
- [29] Levi E, Barrero F, Duran MJ. Multiphase Machines and Drives-Revisited. *IEEE Transactions On Industrial Electronics* 2016; 63(1): 429-432.
- [30] Liu Z, Li Y, Zheng Z. A Review of Drive Techniques for Multiphase Machines. *Ces Transactions On Electrical Machines And Systems* 2018; 2(2): 243-251.
- [31] Pantea A, Yazidi A, Betin F, Taherzadeh M, Carriere S, Henao H, Capolino G.A. Six-Phase Induction Machine Model for Electrical Fault Simulation Using the Circuit-Oriented Method. *IEEE Transactions On Industrial Electronics* 2016; 63(1): 494-503.
- [32] Pandit JK, Aware VA, Nemade RV, Levi E. Direct Torque Control Scheme for a Six-Phase Induction Motor With Reduced Torque Ripple. *IEEE Transactions On Power Electronics* 2017; 32(9): 7118-7129.
- [33] Munim WNWA, Duran MJ, Che HS, Bermudez M, Ignacio GP, Rahim NA. A Unified Analysis of the Fault Tolerance Capability in Six-Phase Induction Motor Drives. *IEEE Transactions On Power Electronics* 2017; 32(10): 7824-7836.
- [34] Che HS, Abdel-Khalik AS, Dordevi, O, Levi E. Parameter Estimation of Asymmetrical Six-Phase Induction Machines Using Modified Standard Tests. *IEEE Transactions On Industrial Electronics* 2017; 64(8): 6075-6085.
- [35] Pandit JK, Awar, MV, Nemade R, Tatte, Y. Simplified Implementation of Synthetic Vectors for DTC of Asymmetric Six-Phase Induction Motor Drives. *IEEE Transactions On Industry Applications* 2018; 54(3): 2306-2318.
- [36] Holakooie MH, Ojaghi M, Taheri A. Direct Torque Control of Six-Phase Induction Motor With a Novel MRAS-Based Stator Resistance Estimator. *IEEE Transactions On Industrial Electronics* 2018; 65(10): 7685-7696.
- [37] Holakooie MH, Ojaghi M, Taheri A. Modified DTC of a Six-Phase Induction Motor With a Second-Order Sliding-Mode MRAS-Based Speed Estimator. *IEEE Transactions On Power Electronics* 2019; 34(1): 600-611.
- [38] Abdel-Khalik AS, Hamdy RA, Massoud AM, Ahmed S. Low-Order Space Harmonic Modeling of Asymmetrical Six-Phase Induction Machines. *IEEE Access* 2019; 7: 6866-6876.
- [39] Bojoi R, Lazzari M, Profumo F, Tenconi A, Digital Field-Oriented Control for Dual Three-Phase Induction Motor Drives. *IEEE Transactions on Industry Applications* 2003; 39(3): 752-760.
- [40] Gündoğdu A., “Torque Ripple Reduction of Asynchronous Motor by Neural-Fuzzy Networks”, Phd.Thesis, Firat University Institute of Science, Elazığ, Turkey, 2012.
- [41] Uzun H, Akar O, Demirci A, Akuner MC, Terzi UK. Analyzing High Efficiency Asynchronous Motors Using Scalar Control Technique. *Balkan Journal of Electrical & Computer Engineering* 2018; 6: 23-26.